

'Senescence-associated vacuoles' are involved in the degradation of chloroplast proteins in tobacco leaves

Dana E. Martínez^{1,†}, María L. Costa^{1,†}, Facundo M. Gomez¹, Marisa S. Otegui² and Juan J. Guiamet^{1,*}

¹Instituto de Fisiología Vegetal, Universidad Nacional de La Plata, cc 327, 1900 La Plata, Argentina, and

²Department of Botany, University of Wisconsin, 224 Birge Hall, Madison, WI 53706, USA

Received 9 April 2008; accepted 9 May 2008; published online 15 August 2008.

*For correspondence (fax +54 221 4233698; e-mail jguiamet@fcnym.unlp.edu.ar).

†These authors contributed equally to this paper.

Summary

Massive degradation of photosynthetic proteins is the hallmark of leaf senescence; however the mechanism involved in chloroplast protein breakdown is not completely understood. As small 'senescence-associated vacuoles' (SAVs) with intense proteolytic activity accumulate in senescing leaves of soybean and Arabidopsis, the main goal of this work was to determine whether SAVs are involved in the degradation of chloroplastic components. SAVs with protease activity were readily detected through confocal microscopy of naturally senescing leaves of tobacco (*Nicotiana tabacum* L.). In detached leaves incubated in darkness, acceleration of the chloroplast degradation rate by ethylene treatment correlated with a twofold increase in the number of SAVs per cell, compared to untreated leaves. In a tobacco line expressing GFP targeted to plastids, GFP was re-located to SAVs in senescing leaves. SAVs were isolated by sucrose density gradient centrifugation. Isolated SAVs contained chloroplast-targeted GFP and the chloroplast stromal proteins Rubisco (ribulose-1,5-bisphosphate carboxylase/oxygenase) and glutamine synthetase, but lacked the thylakoid proteins D1 and light-harvesting complex II of the photosystem II reaction center and photosystem II antenna, respectively. In SAVs incubated at 30°C, there was a steady decrease in Rubisco levels, which was completely abolished by addition of protease inhibitors. These results indicate that SAVs are involved in degradation of the soluble photosynthetic proteins of the chloroplast stroma during senescence of leaves.

Keywords: senescence-associated vacuoles, proteolysis, chloroplast breakdown, Rubisco, glutamine synthetase, tobacco.

Introduction

Leaf senescence is a programmed dismantling process during which cellular structures are broken down, and the released nutrients are remobilized for re-use in other parts of the plant (Noodén *et al.*, 2004). Although this remobilization contributes nitrogen and other nutrients for seed growth, the concomitant drop in photosynthetic activity limits the yield potential of several important crops (Thomas and Howarth, 2000; Tollenaar and Wu, 1999). On a global scale, billions of tons of chlorophyll (Hendry *et al.*, 1987) and photosynthetic proteins are degraded during the senescence of leaves every year. However, despite the massive amounts of protein involved (arguably chloroplasts contain the largest single pool of protein on Earth), the mechanism(s) responsible for chloroplast protein degradation in senescing leaves remains unclear (Feller *et al.*, 2008; Krupinska, 2006; Martínez *et al.*, 2008).

Various mechanisms have been proposed to account for chloroplast degradation during senescence (Hörtensteiner and Feller, 2002). One model postulates that chloroplast components (e.g. photosynthetic proteins) are degraded by hydrolytic enzymes (e.g. chloroplast-targeted proteases) within the chloroplasts of senescing leaves. An alternative hypothesis states that chloroplast components are somehow exported to the central vacuole, or other lytic compartment(s) (Hörtensteiner and Feller, 2002). The possibility that the photosynthetic machinery is degraded *in situ* by chloroplast-localized hydrolases is supported by the finding that the initial steps of chlorophyll breakdown are catalyzed by chloroplast enzymes (Hörtensteiner, 2006). Proteases of the Clp, FtsH and DegP families are expressed in chloroplasts, and representatives of these proteases are up-regulated in senescing leaves (Adam and Clarke, 2002; Andersson *et al.*,

2004; Gepstein *et al.*, 2003; Nakabayashi *et al.*, 1999). Recently, the chloroplast aspartic protease CND41 was implicated in Rubisco degradation (Kato *et al.*, 2004), although this may represent an indirect effect as CND41 is also involved in regulating gibberellin homeostasis and growth (Nakano *et al.*, 2003). Plastids isolated from senescing leaves can degrade photosynthetic proteins to some extent, particularly under light (Feller, 2004; Feller *et al.*, 2008). However, isolated chloroplasts seem to be incapable of completing the degradation of Rubisco (the most abundant photosynthetic protein) beyond an initial cleavage of its N-terminus (Kokubun *et al.*, 2002; Zhang *et al.*, 2007). At present, there are no good candidate chloroplastic proteases that might account for the degradation of most photosynthetic proteins during senescence.

Various studies have identified genes whose expression increases in senescing leaves (i.e. 'senescence-associated genes', SAGs), and many of these genes encode hydrolytic enzymes (Buchanan-Wollaston *et al.*, 2003), including vacuolar proteases (e.g. Drake *et al.*, 1996). Vacuolar cysteine proteases increase in activity during the senescence of wheat leaves (Martínez *et al.*, 2007). In addition, vacuolar-processing enzymes, a subset of cysteine proteases involved in maturation of vacuolar proteins, are up-regulated in senescing leaves of several species (Kinoshita *et al.*, 1999; Smart *et al.*, 1995). N-terminally cleaved fragments of the large subunit of Rubisco accumulate during senescence under certain conditions (e.g. dark incubation of excised leaves), but these fragments are not produced by chloroplast lysates, suggesting that hydrolases outside the plastid might play a role in the degradation of chloroplast components (Feller *et al.*, 2008).

We have previously described a novel class of lytic vacuoles in senescing leaves of soybean and *Arabidopsis thaliana* (Otegui *et al.*, 2005). These 'senescence-associated vacuoles' (SAVs) are small (0.5–0.8 µm diameter), and are clearly distinguishable from the central vacuole with respect to their luminal pH (SAVs are more acidic) and tonoplast composition. SAVs exhibit high proteolytic activity *in vivo*. Intriguingly, SAVs develop in the chloroplast-containing mesophyll and guard cells of the leaf, whereas non-green epidermal cells lack SAVs. As SAVs occur in senescing leaves, develop in chloroplast-containing cells and have high proteolytic activity, we hypothesized that SAVs might be involved in the degradation of chloroplast proteins during senescence. In this paper, we combine *in vivo* observations by confocal microscopy with isolation and biochemical analysis of SAVs to show that chloroplast components (e.g. chloroplast-targeted GFP, Rubisco and chloroplastic glutamine synthetase) are found in SAVs of senescing leaves, and that isolated SAVs can degrade Rubisco. These observations support the idea that SAVs are a specific class of vacuoles involved in degradation of the photosynthetic machinery during senescence of leaves.

Results

Senescence-associated vacuoles in tobacco

Senescence-associated vacuoles of *Arabidopsis* and soybean are easily detected by confocal microscopy of live cells incubated with the vacuolar markers Neutral Red or LysoTracker Red (Otegui *et al.*, 2005). SAVs can also be distinguished from the central vacuole because of their smaller size (0.5–0.8 µm diameter). Similar small vacuoles were detected using LysoTracker Red in senescing leaves of tobacco (Figure 1). In herbaceous species, leaves senesce in a sequential pattern from the base upwards as apical growth gives rise to new leaves on top of the plant. Under our conditions, the first leaves from the bottom (i.e. leaves 1–3, Figure 1a) showed clear signs of senescence (i.e. decreased chlorophyll, protein and Rubisco levels, Figure 1b), whereas upper younger leaves (leaves 6–10, Figure 1a) contained higher levels of these photosynthetic components (Figure 1b). SAVs were not detectable in leaf pieces excised from young leaves (leaf 7, Figure 1c), whereas numerous SAVs were easily seen in senescing leaves (leaves 1–3, Figure 1c).

SAVs of *Arabidopsis* and soybean are characterized by intense proteolytic activity (Otegui *et al.*, 2005). To determine whether tobacco SAVs likewise contain active proteases, and to advance characterization of the classes of proteases present in SAVs, we incubated cells isolated from senescing leaves with two fluorescent probes for peptidase activity, R6502 and R6505, which are reported to be specific substrates for cysteine and serine proteases, respectively (<http://www.probes.com>). These bis-amide probes have a very low fluorescence yield, but become brightly fluorescent upon hydrolysis of the amide moiety by peptidases. Tobacco SAVs showed activity towards R6502 and R6505, indicating that they contain active cysteine and serine proteases (Figure S1).

Chloroplast-targeted GFP re-localizes to SAVs

As SAVs occur in the chloroplast-containing cells of the leaf (Otegui *et al.*, 2005), we surmised that they might be involved in the degradation of chloroplast components, and therefore that it might be possible to detect a chloroplast-targeted protein in SAVs. To do this, we used a tobacco line expressing GFP fused to a chloroplast targeting sequence (TP-GFP, Köhler *et al.*, 1997) and assessed the GFP signal in SAVs. Immunoblot analysis of the changes in GFP levels showed that GFP content started to decrease in leaves 3 and 4 (Figure 2). The decline in GFP levels paralleled the senescence-associated decrease in abundance of the large subunit of ribulose-1,5-bisphosphate carboxylase/oxygenase (Rubisco), making TP-GFP a useful surrogate of chloroplast proteins. In mature, non-senescent leaves of the TP-GFP

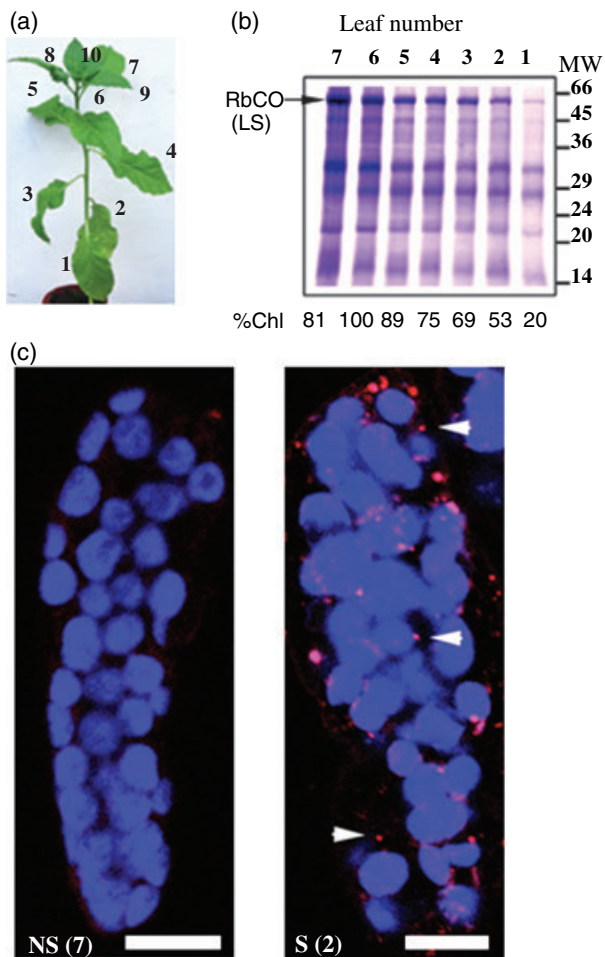


Figure 1. Senescence-associated vacuoles (SAVs) in leaves of wild-type tobacco.

(a) Tobacco leaves senesce sequentially from the base towards the top of the plant. Leaves were numbered as they emerged on the plant. Leaves 1–3, senescing leaves; leaves 4–7, mature, fully expanded leaves; leaves 8–10, young leaves.

(b) Coomassie blue-stained SDS-PAGE gel showing the changes in leaf protein content during senescence. Lane numbers correspond to leaf numbers. Each lane was loaded with protein representing 11 mm² of leaf area. The position of molecular mass markers is shown on the right. An arrow shows the position of Rubisco large subunit (RbCO LS).

(c) Confocal images (1 μm thick optical sections) of cells from senescing [S(2), leaf 2] and mature, non-senescent [NS(7), leaf 7] leaves of tobacco. Cells were isolated and incubated with LysoTracker Red to label SAVs. Arrowheads show typical SAVs. LysoTracker Red is pseudocolored red; chlorophyll autofluorescence is shown in blue. Scale bar = 10 μm.

line, GFP localized with chlorophyll autofluorescence, i.e. GFP was correctly targeted to plastids (Figure 3a). No GFP signal outside plastids was seen in mature, non-senescent leaves of the TP-GFP line (Figure 3a). In contrast, the GFP signal of TP-GFP appeared to be re-located to SAVs in senescing leaves. Figure 3(b) shows a typical senescent leaf cell with many SAVs (labeled by LysoTracker Red) containing a clear GFP signal. Control observations showed that this

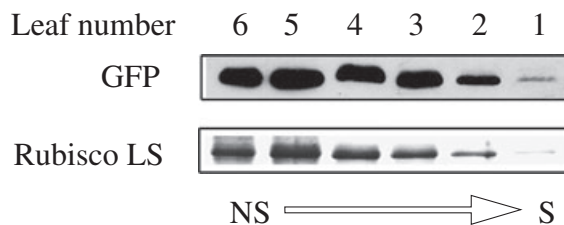


Figure 2. Changes in GFP protein content throughout leaf development in a tobacco line expressing GFP fused to a chloroplast targeting sequence (TP-GFP). Upper panel: immunodetection of GFP. Lower panel: Coomassie blue-stained Rubisco large subunit. Leaves are numbered from the bottom of the plant (from senescing leaf 1 to the younger, non-senescent leaf 6). Protein extracted from 11 mm² of leaf area was loaded in each lane.

signal derived from GFP, as there was no detectable autofluorescence in this region of the spectrum in wild-type cells (data not shown). To confirm the identity of the fluorescence signal arising from SAVs, we determined the fluorescence emission spectra in the GFP range (494–558 nm) for SAVs and chloroplasts of TP-GFP leaves. These fluorescence emission spectra were identical (Figure 3c), confirming that the signal in SAVs represents GFP. It is important to note that we could not detect physical connections between GFP-containing SAVs and chloroplasts in cells that were scanned through overlapping optical slices covering 4 μm around the plane of selected SAVs (Figure S2).

Chlorophyll autofluorescence in SAVs

Some SAVs of wild-type (data not shown) and TP-GFP plants (Figure 3b) displayed a fluorescence signal in the 670–730 nm region of the spectrum, which may represent chlorophyll autofluorescence. Spectral analysis of fluorescence emission in the 650–730 nm range showed that the fluorescence signal arising from SAVs was very similar to that of chloroplasts (Figure 3c). SAVs with or without a chlorophyll signal were detected in wild-type leaves (not shown), whereas in TP-GFP plants there were SAVs with GFP and chlorophyll, SAVs with only GFP but no chlorophyll, and a few SAVs with neither GFP nor chlorophyll (Figure 3b).

The number of SAVs correlates with the chloroplast degradation rate

The rate of chloroplast degradation during senescence can be modulated by hormone treatments, with ethylene typically accelerating the loss of chloroplast components (e.g. John *et al.*, 1995). Excised leaves of TP-GFP tobacco incubated in continuous darkness lost little chlorophyll in 2 days, whereas leaves incubated under the same conditions but treated with the ethylene-releasing compound ethephon lost approximately 30% (Figure S3). These differences in the

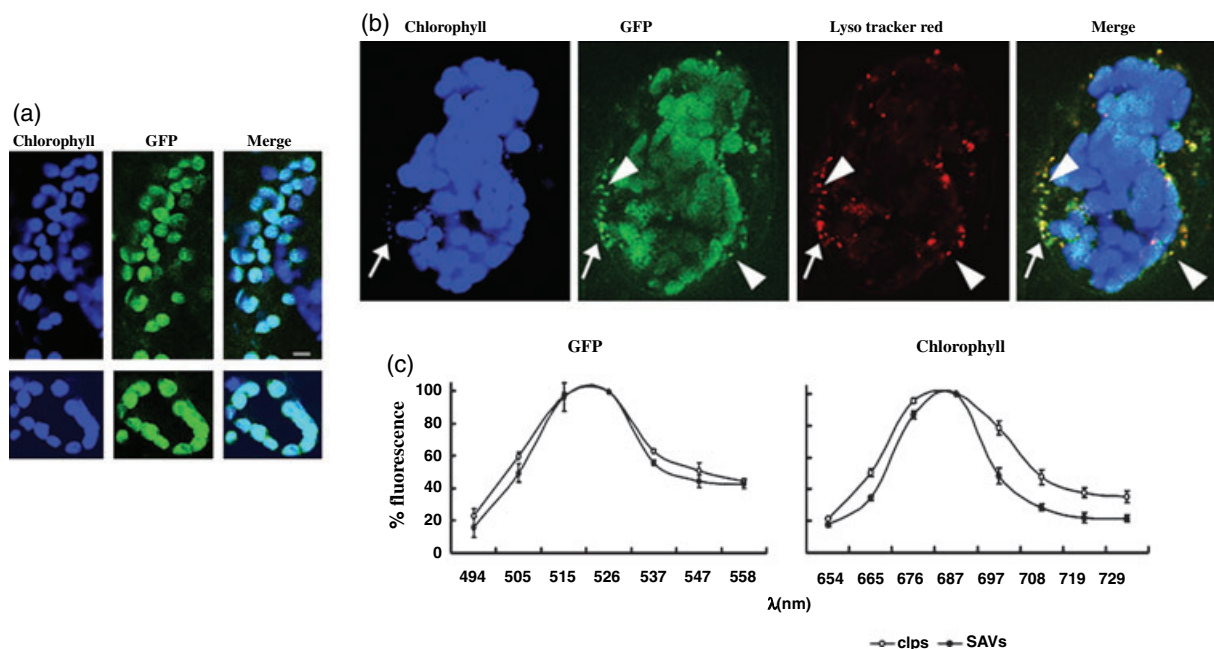


Figure 3. SAVs in senescing leaves of TP-GFP tobacco.

(a) GFP detection in cells of non-senescent, mature leaves of a transgenic tobacco line expressing GFP fused to a chloroplast-targeting sequence (TP-GFP). Confocal images (1 μm thick optical sections) of cells isolated from a young leaf (leaf 6). Scale bar = 5 μm .

(b) Confocal section (1 μm thick) through a cell isolated from a senescing leaf expressing TP-GFP and incubated with LysoTracker Red. The punctate pattern of the GFP signal outside chloroplasts localizes to SAVs labeled with LysoTracker Red (arrowheads). Less frequently, a fluorescence signal with spectral properties of chlorophyll is also detected in SAVs (arrows show SAVs with GFP and chlorophyll fluorescence). Scale bar = 5 μm .

(c) Emission spectra of SAVs and chloroplasts (clps) in the GFP and chlorophyll fluorescence wavelength bands. Excitation wavelengths were 488 nm and 633 nm for GFP and chlorophyll, respectively. Curves were normalized to the maximum fluorescence intensity for each spectrum. Values represent the means from six chloroplasts and eight SAVs. Vertical bars represent the standard error of the mean. Open circles, chloroplasts (clps); closed circles, SAVs.

rates of chloroplast degradation correlated with the abundance of SAVs, with many more SAVs in cells of ethephon-treated leaves (Table 1 and Figure S4). The mean number of SAVs in a 1 μm thick optical section increased approximately twofold in leaves treated with ethephon. The percentage of SAVs with a detectable GFP signal was approximately the same (45–50%) in control and ethephon-treated cells (data not shown). Interestingly, SAVs from ethephon-treated leaves mostly lacked the fluorescence signal in the 670–730 nm band corresponding to chlorophyll autofluorescence (data not shown).

Table 1 Abundance of SAVs in detached leaves incubated in darkness for 2 days, and treated with the ethylene-releasing compound ethephon

	Darkness	Darkness plus ethephon
Number of SAVs per cell section	26 \pm 4 ^a	61 \pm 6 ^b
Number of chloroplasts per cell section	43 \pm 4 ^a	42 \pm 6 ^a

SAVs and chloroplasts were counted in six cells per treatment; each cell was examined over three non-consecutive optical sections (1 μm thick each). Values are means \pm SEM. Means followed by different letters are significantly different at $P < 0.01$.

Chloroplast proteins in isolated SAVs

To advance our understanding of the composition of SAVs, we isolated SAVs from TP-GFP leaves treated with ethephon and induced to senesce in darkness for 2 days. Based on our confocal microscopy observations, we reasoned that an SAV-enriched fraction should concentrate the acidotropic dye Neutral Red (NR). Therefore, a crude leaf extract was incubated with NR for 15 min, chloroplasts were pelleted by low-speed centrifugation, and the supernatant was fractionated by sucrose density centrifugation. A red band at approximately 26% sucrose contained numerous SAVs, which were readily detected by their staining with NR and GFP signal (Figure 4a,b); this band was devoid of chloroplasts. Simultaneous imaging of isolated SAVs by differential interference contrast (DIC) and NR fluorescence showed that all membrane structures collected in our preparation were labeled by NR, i.e. there were no other organelles or vesicles in addition to those labeled by NR (Figure 4c,d). Immunoblot analysis of the fractions separated show that V-H⁺ pyrophosphatase (previously shown to label SAVs, Otegui *et al.*, 2005) and GFP peaked with the NR-containing band at 26% sucrose (Figure 5a). The SAV fraction banding at 26% sucrose was treated with thermolysin to remove proteins

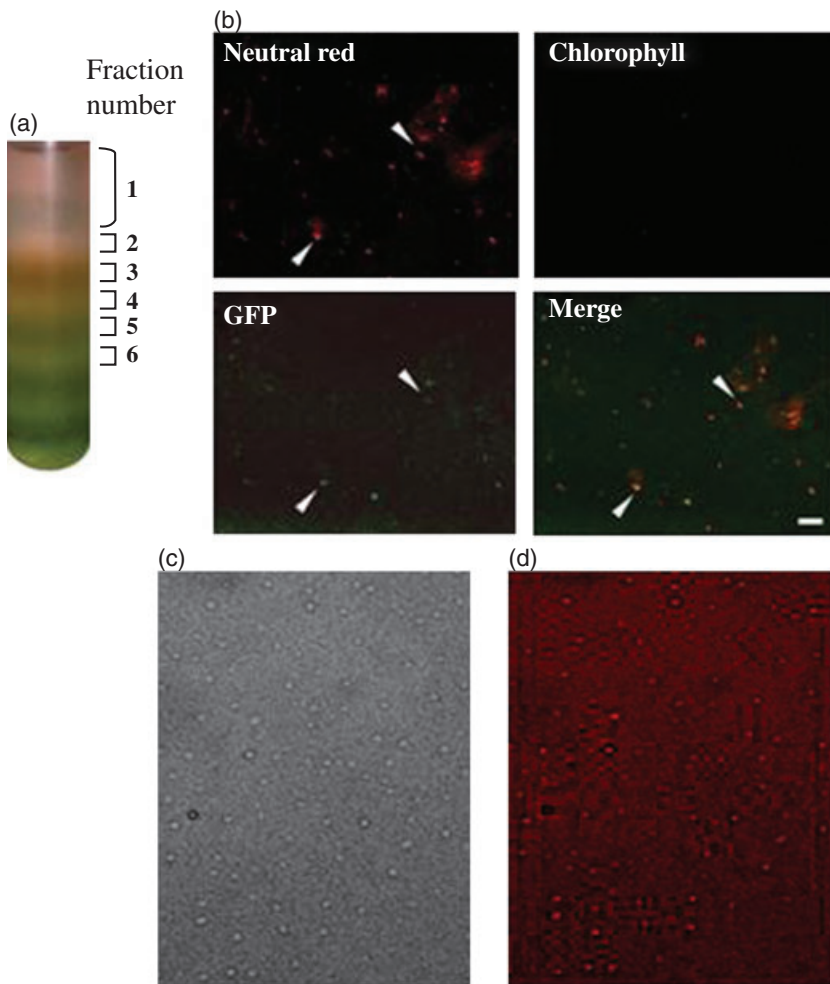


Figure 4. Isolation and microscopic analysis of an SAV-enriched fraction.

(a) Homogenates from senescing leaves of tobacco expressing TP-GFP were incubated with Neutral Red, centrifuged at 2500 *g* to pellet chloroplasts, and then the supernatant was fractionated on a discontinuous sucrose density gradient (5%, 25%, 35% and 60% w/v sucrose). (b) Confocal fluorescence image of the SAV-enriched fraction. Fraction 3 from the sucrose gradient (a) was fixed with formaldehyde, and examined by confocal fluorescence microscopy. Scale bar = 10 μ m.

(c, d) Fresh (non-fixed) preparation of SAVs viewed by DIC (c), and a merged image of DIC and Neutral Red fluorescence (d).

outside the SAVs, the thermolysin was then inactivated with EGTA, and SAVs were purified again in the same sucrose density gradient (Figure 5b) and analyzed by Western blotting. Consistent with previous immunolocalization data, the SAV fraction contained vacuolar H^+ -pyrophosphatase, but lacked the central vacuole aquaporin γ -TIP (Otegui *et al.*, 2005) (Figure 5c). Isolated SAVs were mostly devoid of cytochrome *c*, catalase, glutamine synthetase 1 (GS1) and aryl mannosidase activity, markers for mitochondria, peroxisomes, cytosol and the Golgi complex, respectively (Figure 5c). The ER marker protein BiP peaked at higher sucrose concentrations than SAVs did (Figure 5a). SAVs from ethephon-treated leaves did not contain either the photosystem II reaction center protein D1 or the chlorophyll *a/b* binding proteins associated with the antenna of photosystem II (Figure 5c), which provides biochemical confirmation that the SAV fraction was not contaminated by chloroplasts or chloroplast fragments.

SAVs isolated from leaves of TP-GFP plants contained GFP (Figures 4a and 5a) and high levels of the large subunit of Rubisco (Figure 5c). Similarly, a significant amount of

chloroplastic glutamine synthetase (GS2) (Scarpeci *et al.*, 1997) could be detected in SAVs. As SAVs were treated with thermolysin and then re-isolated, we can rule out the possibility that chloroplast proteins might be co-migrating with SAVs, rather than actually being inside these vacuoles. As a control, we show that Rubisco is extensively degraded by thermolysin if SAVs are lysed by prior addition of Triton X-100 (Figure S5), indicating that Rubisco is protected from thermolysin attack by the limiting membrane of SAVs. Thus, SAVs contain substantial amounts of stromal proteins of the chloroplast (i.e. Rubisco and chloroplastic GS2), but lack the membrane proteins of photosystem II.

Chloroplast protein degradation within SAVs

The presence of chloroplast stromal proteins in SAVs prompted us to test whether chloroplast proteins can be degraded within SAVs. We followed the changes in the levels of Rubisco large subunit in isolated SAVs incubated at 30°C. A significant amount of Rubisco large subunit was degraded within 4 h of incubation at pH 5.5 (Figure 6a), and

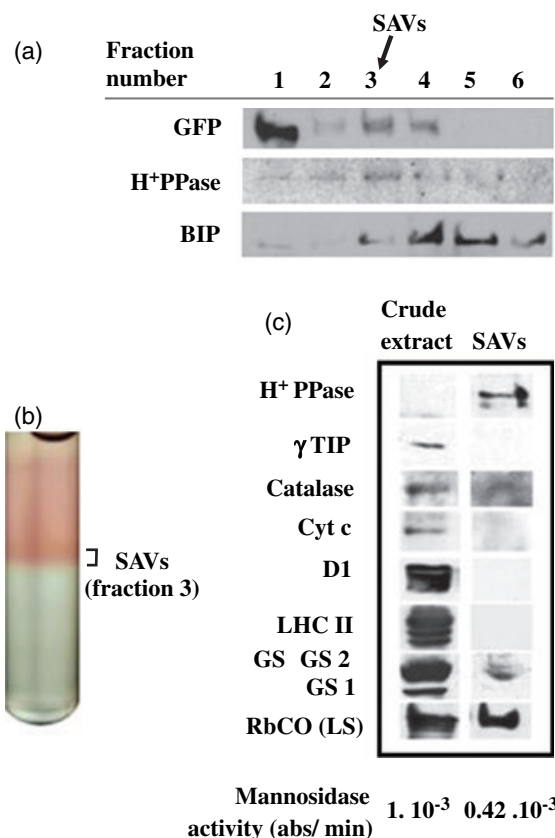


Figure 5. Biochemical characterization of isolated SAVs.

(a) Western blot analysis of sucrose density gradient fractions probed with anti-GFP, V-H⁺-pyrophosphatase (PPase) and BiP antibodies. Aliquots (40 μl) of each fraction [shown in (b)] were loaded in each lane. The peak contents of V-H⁺-PPase and GFP in fraction 3 represent biochemical evidence for SAV enrichment, and are consistent with the presence of GFP and Neutral Red in the same fraction (Figure 4b). The percentage sucrose content in each fraction was measured using a refractometer after ultracentrifugation.

(b) Sucrose density gradient centrifugation of the SAV-enriched fraction after thermolysin treatment.

(c) Western blot analysis of isolated SAVs. Aliquots (25 μg) of protein from the crude leaf homogenate and the SAV-enriched fraction were analyzed by Western blotting. V-H⁺-PPase was detected in the SAV-enriched fraction, which was devoid of γ-TIP, catalase and cytochrome c (cyt c), markers for the central vacuole, peroxisomes and mitochondria, respectively. The activity of aryl mannosidase, a Golgi marker, is much lower in SAVs than in the crude extract. The thylakoid proteins D1 and LHCII were not detected in SAVs. The SAV-enriched fraction contains the stromal, chloroplast-encoded large subunit of Rubisco and chloroplastic glutamine synthetase (GS2). The anti-GS antibody also detects the cytosolic GS1 isoform (with a lower apparent molecular mass), which is absent from SAVs.

this degradation was completely abolished in SAVs treated with a mixture of protease inhibitors (Figure 6b).

Chlorophyll a in isolated SAVs

An HPLC analysis of pigments showed the presence of chlorophyll a in SAVs isolated from leaves induced to senesce in darkness, with no ethephon treatment (Figure 7). This SAV preparation lacked the D1 protein of

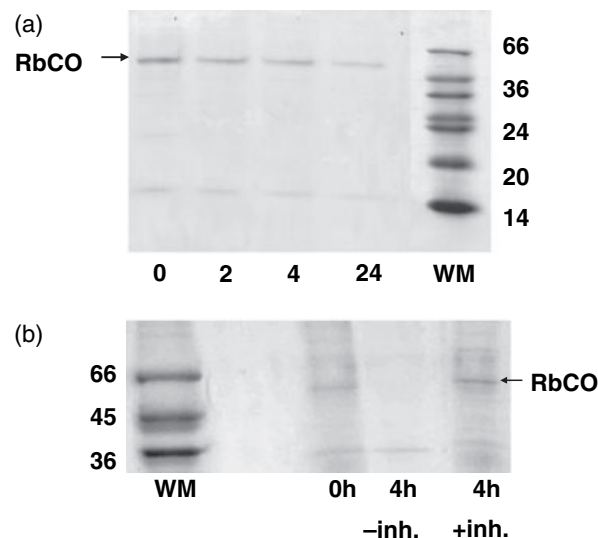


Figure 6. Rubisco degradation in isolated SAVs.

(a) An SAV-enriched fraction (treated with thermolysin and re-isolated as described in Experimental procedures) was incubated at 30°C for up to 24 h. Equal aliquots of the SAV-enriched fraction were sampled at 0, 2, 4 and 24 h of incubation and analyzed by SDS-PAGE and Coomassie blue staining.

(b) Inhibition of Rubisco degradation by a mixture of protease inhibitors (+ inh.). RbCO, Rubisco large subunit.

photosystem II (data not shown), ruling out the possibility that the presence of chlorophyll a in SAVs might be an artifact due to contamination with chloroplasts, chloroplast fragments or thylakoid membranes. These results show that a large proportion of the fluorescence signal in the 670–730 nm range seen in confocal images (Figure 3b,c) may correspond to chlorophyll a.

Discussion

Lytic compartments in senescing organs

The large central vacuole has been traditionally regarded as the lytic organelle of plants (De, 2000); however, senescing cells of a variety of tissues contain lytic compartments other than the central vacuole. For example, small vesicles carrying the pro-enzyme form of the CysEP protease (i.e. ricinosomes) have been described in senescing endosperm cells of *Ricinus communis* (Schmid *et al.*, 1999). Cells in the aleurone layer of barley seeds develop small, acidic and proteolytically active secondary vacuoles after seed germination (Swanson *et al.*, 1998). SAVs are a novel lytic compartment of senescing leaves. The presence of two types of lytic vacuoles (i.e. SAVs and the central vacuole) in senescing leaf cells seems paradoxical. However, SAVs are 0.8 pH units more acidic than the central vacuole (Otegui *et al.*, 2005), and *in vivo* experiments show that small changes in vacuolar pH can greatly affect proteolytic activity (Hwang *et al.*, 2003; Moriyasu, 1995). Thus, maintaining a very acidic

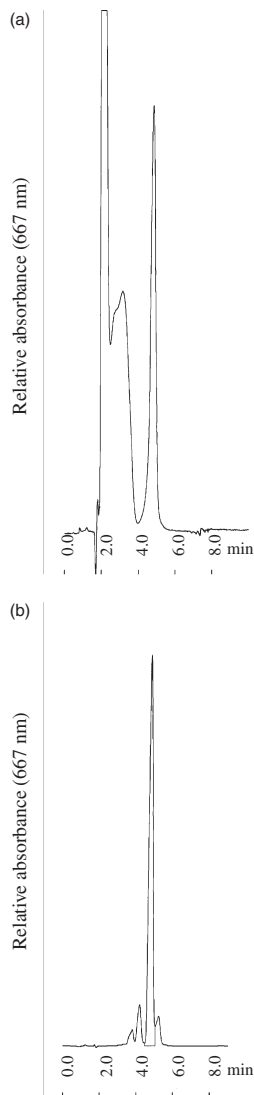


Figure 7. Detection of chlorophyll *a* in isolated SAVs. (a) HPLC chromatogram of pigments extracted from SAVs isolated from leaves induced to senescence in darkness. (b) Chlorophyll *a* standard. Note the peak in (a) that shows the same retention time as pure chlorophyll *a*.

environment may be a prerequisite for protein degradation in vacuoles, and it may be energetically less costly to maintain a very low pH in SAVs than in the much larger central vacuole.

Chloroplast proteins in SAVs

An important goal of this work was to determine whether SAVs contain chloroplast proteins, and therefore whether SAVs might be involved in their breakdown. *In vivo* observations show that chloroplast-targeted GFP re-localizes to SAVs during senescence of TP-GFP tobacco leaves. We also detected the chloroplast-encoded large subunit of Rubisco

and chloroplastic glutamine synthetase in isolated SAVs. The fact that SAVs contain chloroplast proteins and have high peptidase activity suggests that these vacuolar compartments are lytic organelles involved in the degradation of some chloroplast proteins. Small, extra-plastidial, spherical bodies containing the large subunit of Rubisco and chloroplastic glutamine synthetase, but not thylakoid proteins, were found in the cytosol of senescing leaves of wheat (Chiba *et al.*, 2003). Unlike SAVs, which are surrounded by a single membrane (Otegui *et al.*, 2005), these 'Rubisco-containing bodies' (RCBs) are bound by a double membrane, and it is not known whether they represent a lytic compartment (i.e. whether they have hydrolytic activities). The relationship, if any, between SAVs and RCBs is presently unknown, but these structures support the possibility that chloroplast proteins can traffic out of the plastid in senescing cells. Protuberances containing Rubisco, but apparently excluding thylakoid membranes, protrude from chloroplasts of C_3 species (Bourett *et al.*, 1999). Both SAVs and RCBs seem to contain primarily soluble stromal proteins, and may arise from scission of these chloroplast bulges. It is interesting that cytosolic vacuoles of *Chlamydomonas* cells contain chloroplast proteins (Park *et al.*, 1999), and ultrastructural studies suggest that these vacuoles might originate from fusion of Golgi-derived vesicles with chloroplast contents extruded from chloroplast protuberances (Park *et al.*, 1999). Detailed ultrastructural studies may help to understand the biogenesis of SAVs.

Rubisco degradation in SAVs

The findings that (i) SAVs contain photosynthetic proteins, (ii) SAVs are proteolytically active, and (iii) SAVs can degrade their Rubisco content *in vitro*, are strong evidence supporting a role for SAVs in the degradation of photosynthetic proteins. However, the absence of D1 and light-harvesting complex II (LHCII) in SAVs suggests that not all photosynthetic proteins are degraded in these organelles. Degradation of D1 may present a special case. Regardless of the developmental stage of the leaf, D1 has a very high turnover rate, and is rapidly broken down and re-synthesized as part of a photo-inhibition repair mechanism (Aro *et al.*, 1993). Chloroplastic DegP and FtsH proteases appear to cooperate in D1 degradation during photo-inhibition (Kapri-Pardes *et al.*, 2007), and it seems likely that they might also be responsible for D1 degradation during senescence. Likewise, there is evidence that LHCII degradation is carried out by the chloroplastic FtsH6 protease (Zelisko *et al.*, 2005). Unlike thylakoid proteins, degradation of Rubisco within senescing chloroplasts appears to be relatively slow (compared to the high rates in isolated SAVs), and may not progress beyond initial N-terminal cleavage of the large subunit (Kokubun *et al.*, 2002; Zhang *et al.*, 2007). Thus, SAVs may function in breakdown of the stromal, soluble proteins of the chloroplast

(e.g. Rubisco and glutamine synthetase), while proteins of the photosynthetic membranes might be degraded through other pathways operating within the plastid. This is consistent with genetic and biochemical evidence showing that degradation of Rubisco and LHClI proteins can be influenced separately by environmental conditions (Hidema *et al.*, 1991, 1992), or affected independently of each other by genetic mutations (Guamét and Gianibelli, 1996; Guamét *et al.*, 1991; Kusaba *et al.*, 2007). Although our data indicate that SAVs are involved in breakdown of the stromal proteins of the chloroplast, we cannot rule out the operation of alternative/additional degradation pathways within the plastid. A breakdown mechanism where proteins are first exported out of the plastid may seem unnecessarily complicated, but SAVs may provide an optimum environment for proteolysis (e.g. low pH), while allowing conditions within the plastid to remain undisturbed and permit the remaining photosynthetic apparatus to operate normally. As the concentration of amino acids in the central vacuole increases during senescence of leaves (Matile, 1997), a degradation pathway involving SAVs might eventually result in fusion of SAVs to the central vacuole, where amino acids resulting from protein degradation might be temporarily stored before remobilization to other parts of the plant.

A better understanding of the biogenesis of SAVs and the trafficking of stromal proteins from chloroplasts to SAVs, together with identification of SAV hydrolases, might help to identify potential targets for manipulation of protein degradation in senescing leaves.

Chlorophyll degradation in SAVs?

Consistently, a fraction of SAVs contained chlorophyll *a*. The known pathway for chlorophyll degradation in senescing leaves involves a series of reactions that eventually lead to the formation of colorless catabolites that are stored in the central vacuole (Hörtensteiner, 2006). The first steps in this pathway, catalyzed by chlorophyllase, a metal-chelating substance and pheophorbide *a* oxygenase, occur within plastids (Hörtensteiner, 2006). The data presented in this paper do not contradict the operation of chlorophyll degradation within the plastid. However, the presence of chlorophyll *a* in SAVs implies that there may be alternative non-plastidic pathways for chlorophyll degradation, as suggested previously by the cloning of non-chloroplastic chlorophyllases in *Arabidopsis* and *Chenopodium* (Takamiya *et al.*, 2000). Chlorophyll *a* was detected in SAVs of leaves senescing at a relatively slow rate (i.e. without ethephon treatment) but not in leaves treated with ethephon, which may suggest that degradation of chlorophyll occurs within SAVs only under certain conditions. A thorough analysis of chlorophyll catabolites and chlorophyll-binding proteins contained in SAVs will allow determination of the role of SAVs in chlorophyll degradation during senescence, and the

possible contribution of extra-plastidic pathways to pigment breakdown.

Experimental procedures

Plant material and growing conditions

Plants of tobacco (*Nicotiana tabacum* L. cv. Xanthi NN or line TP-GFP) were grown in pots containing soil in a growth chamber at 24/18°C day/night temperature, 300 $\mu\text{mol m}^{-2} \text{sec}^{-1}$ of photosynthetically active radiation and a 10 h photoperiod. TP-GFP expresses the green fluorescent protein (GFP) fused to the transit peptide from the *Arabidopsis* chloroplast *recA* gene driven by a double CaMV 35S promoter (Köhler *et al.*, 1997). TP-GFP was in the background of cv. Petit Havana.

Senescence manipulation by darkness and ethylene treatment

In some experiments, mature leaves were detached, placed on moist filter paper in Petri dishes, and induced to senesce in continuous darkness for 2–3 days at 24°C. Other leaves were treated by immersion for 3 min in ethephon (100 ppm) dissolved in DMSO (0.1% v/v). Control leaves were treated with DMSO (0.1% v/v).

Cell isolation

Leaves were sectioned into small pieces (1 mm wide) and digested with pectolyase (0.3% w/v dissolved in 25 mM MES buffer pH 5.5, 0.5 M mannitol) at room temperature for 2 h. Isolated cells were filtered through four layers of gauze and collected by low speed (50 *g*) centrifugation. Cells were washed four or five times with fresh buffer (25 mM MES pH 6.2, 0.5 M mannitol) without pectolyase.

Fluorescent probes

R6502 (rhodamine 110, bis-CBZ-L-phenylalanyl-L-arginine amide), R6505 (rhodamine 110, bis-CBZ-L-isoleucyl-L-prolyl-L-arginine amide) and LysoTracker Red (Molecular Probes Inc., <http://www.probes.invitrogen.com>) were dissolved in MES buffer (25 mM pH 6.2) and used at concentrations of 0.5 μM (LysoTracker Red) or 50 μM (R6502 and R6505). Leaf pieces or isolated cells were incubated with probes for 20–40 min, and the excess dye was washed with fresh buffer before observation.

Laser scanning confocal microscopy

Leaf pieces or isolated cells were observed under a Zeiss LSM510 META laser scanning confocal microscope (<http://www.zeiss.com/>). Excitation/emission settings were 488/505–530 nm for GFP, R6502 and R6505, 543/585–615 nm for LysoTracker Red, and 633/670–730 nm for chlorophyll. Experiments using wild-type leaves or cells treated with no fluorescent probe indicated that autofluorescence in the 505–530 and 585–615 nm bands was negligible and did not contribute to the signals recorded for GFP, R6502, R6505 or LysoTracker Red. Additionally, for each fluorophore, we tested whether it might have an emission tail extending into other fluorescence channels. GFP, R6502 and R6505 did not contribute fluorescence in the 585–615 nm region in cells without LysoTracker Red (data not

shown). Likewise, in wild-type control cells, LysoTracker Red showed no fluorescence signal in the 505–530 nm region.

Isolation of SAVs

Approximately 25 g of tobacco leaves were homogenized in 100 ml of buffer (25 mM HEPES pH 7, 0.6 M mannitol, 5 mM cysteine, 2 mM EDTA, 1 mM PMSF, 2 $\mu\text{g ml}^{-1}$ leupeptin, 1% w/v polyvinylpyrrolidone [PVPP]). The homogenate was stirred gently for 15 min in the presence of 0.1 mg ml^{-1} Neutral Red, filtered through a nylon mesh and centrifuged at 2500 g for 5 min to pellet chloroplasts and chloroplast membranes. The supernatant was overlaid on top of a discontinuous sucrose gradient (5, 25, 35, 45 and 60% w/v sucrose prepared in 25 mM HEPES pH 7, 0.6 M mannitol), and centrifuged at 100 000 g for 1 h at 4°C. To remove contaminating soluble proteins, the fraction enriched in SAVs was treated with thermolysin (60 $\mu\text{g ml}^{-1}$, 0.5 mM CaCl_2) at 4°C for 30 min. Thermolysin treatment was terminated by adding 0.15 mg ml^{-1} EGTA, and SAVs were then re-isolated on a density gradient as described above. Control experiments with bovine albumin as a substrate for thermolysin showed that EGTA treatment completely inhibited thermolysin activity under these conditions (data not shown).

To assay proteolytic activity, SAVs were isolated without protease inhibitors. The pH of the SAV fraction was adjusted to 5.5, and SAVs were incubated at 30°C in darkness. Samples were taken at regular intervals and analyzed by SDS–PAGE. Control experiments were performed using a mix of protease inhibitors (protease inhibitor cocktail for plant cell and tissue extracts, 1% v/v, Sigma-Aldrich Co., <http://www.sigmaaldrich.com/>) added prior to incubation of SAVs.

Fixation and microscopic observation of isolated SAVs

Isolated SAVs were fixed in 3.7% w/v formaldehyde (dissolved in 50 mM HEPES buffer pH 7, 0.5 M mannitol, 5 mM EGTA) for 30 min. Fixed SAVs were pelleted at 12 000 g for 15 min, resuspended in 50 mM HEPES buffer (pH 7, 0.5 M mannitol) and mounted on polylysine-coated glass slides. Confocal microscopy observations were performed using the same settings as indicated above.

For simultaneous observation by DIC and Neutral Red fluorescence, freshly isolated SAVs were imaged with an Evolution VF CCD camera (QImaging, <http://www.qimaging.com>) attached to an Olympus BX61 microscope (<http://www.olympus-global.com/>). For fluorescence observation of Neutral Red, the WG filter (dichroic mirror DM570, excitation filter BP510–550, barrier filter BA590) was used.

Chlorophyll, protein and enzyme analysis

Leaf chlorophyll content was determined non-destructively using an SPAD 502 chlorophyll meter, or after extraction with dimethylformamide as described previously (Inskoop and Bloom, 1985). An HPLC analysis was carried out to detect chlorophyll *a* in SAVs. Isolated SAVs were dissolved in acetone:hexane (1:1 v/v), centrifuged at 16 000 g for 2 min, and the hexane phase was recovered and filtered through a 0.22 μm nylon mesh before injection into an HPLC system. Samples were run in a Chromsep C18 column (<http://www.varianinc.com/>) with a methanol:acetone (80:20 v/v) mixture at a flow rate of 0.7 ml min^{-1} , with detection at 667 nm. Chlorophyll *a* standards were prepared from *Spirulina* sp. as described by Iriyama *et al.* (1974).

Protein content was measured according to the method described by Bradford (1976). Leaves were homogenized in chilled buffer (50 mM HEPES pH 7.6, 1 mM EDTA, 1% w/v PVPP), and centrifuged at 10 000 g for 10 min. For SDS–PAGE analysis, the resulting supernatant was mixed with 2 x solubilization buffer (125 mM Tris pH 6.8, 4% w/v SDS, 10% v/v glycerol, 10% v/v β -mercaptoethanol). SDS–PAGE and Western blotting were carried out as described previously (Martínez *et al.*, 2007). GFP was detected using a monoclonal antibody (Clontech, <http://www.clontech.com/>). Aryl mannosidase activity was measured as described previously Szumilo *et al.* (1986).

Acknowledgements

We thank Dr R. Rivera Pomar (Centro Regional de Estudios Genómicos, Universidad Nacional de La Plata, Argentina) and Dr P. Wappner (Fundación Instituto Leloir, Buenos Aires, Argentina) for allowing us access to their confocal microscopes, Dr E. L. Portiansky (Universidad Nacional de La Plata) for his help with DIC imaging, and Dr S. García Mora and Ms J. Ortega for assistance. We are indebted to Dr M. Hanson (Cornell University, Ithaca, NY) for the gift of TP-GFP seeds, and to Drs M. Maeshima, M. Chrispeels, R. Trelease, A. Mattoo, O. Vallon and E. Valle for the gifts of anti V-H⁺ pyrophosphatase, γ -TIP, BiP, catalase, D1, LHCII and GS antibodies, respectively. This work was funded by Fonda para la Investigación Científica y Tecnológica (Argentina) through PICT 11885. J.J.G. is a researcher at Comisión de Investigaciones Científicas de la Pcia de Buenos Aires (Argentina).

Supporting Information

Additional Supporting Information may be found in the online version of this article.

- Figure S1.** *In vivo* peptidase activity in SAVs from tobacco leaves.
Figure S2. Z-stack (1 μm thick optical slices) covering 4 μm of a senescing mesophyll cell.
Figure S3. Changes in chlorophyll content (SPAD units) in detached leaves of tobacco incubated in darkness and treated with ethephon (100 ppm).
Figure S4. The number of SAVs per cell correlates with chloroplast degradation rates.
Figure S5. Protection of Rubisco large subunit from thermolysin attack in isolated SAVs.
 Please note: Wiley-Blackwell are not responsible for the content or functionality of any supporting materials supplied by the authors. Any queries (other than missing material) should be directed to the corresponding author for the article.

References

- Adam, Z. and Clarke, A.K. (2002) Cutting edge of chloroplast proteolysis. *Trends Plant Sci.* **7**, 451–456.
 Andersson, A., Keskitalo, J., Sjödin, A. *et al.* (2004) A transcriptional timetable of autumn senescence. *Genome Biol.* **5**, R24.
 Aro, E., Virgin, L. and Andersson, B. (1993) Photoinhibition of photosynthesis: inactivation, protein damage and turnover. *Biochim. Biophys. Acta*, **1143**, 113–134.
 Bourett, T.M., Czymbek, K.J. and Howard, R.J. (1999) Ultrastructure of chloroplast protuberances in rice leaves preserved by high-pressure freezing. *Planta*, **208**, 472–479.
 Bradford, M.M. (1976) A rapid and sensitive method for the quantitation of microgram quantities of protein utilizing the principle of protein–dye binding. *Anal. Biochem.* **72**, 248–254.

- Buchanan-Wollaston, V., Earl, S., Harrison, E., Mathas, E., Navabpour, S., Page, T. and Pink, D. (2003) The molecular analysis of leaf senescence – a genomic approach. *Plant Biotechnol. J.* **1**, 3–22.
- Chiba, A., Ishida, H., Nishizawa, N.K., Makino, A. and Mae, T. (2003) Exclusion of ribulose-1,5-bisphosphate carboxylase/oxygenase from chloroplasts by specific bodies in naturally senescing leaves of wheat. *Plant Cell Physiol.* **44**, 914–921.
- De, D.N. (2000) *Plant Cell Vacuoles. An Introduction*. Collingwood, Australia: CSIRO Publishing.
- Drake, R., John, I., Farrell, A., Cooper, W., Schuch, W. and Grierson, D. (1996) Isolation and analysis of cDNAs encoding tomato cysteine proteases expressed during leaf senescence. *Plant Mol. Biol.* **30**, 755–767.
- Feller, U. (2004) Proteolysis. In *Plant Cell Death Processes* (Noodén, L.D., ed.). San Diego, CA: Academic Press, pp. 107–123.
- Feller, U., Anders, I. and Mae, T. (2008) Rubiscolytics: fate of Rubisco after its enzymatic function in a cell is terminated. *J. Exp. Bot.* **59**, 1615–1624.
- Gepstein, S., Sabehi, G., Carp, M.-J., Hajouj, T., Neshet, M.F., Yariv, I., Dor, C. and Bassani, M. (2003) Large-scale identification of leaf senescence-associated genes. *Plant J.* **36**, 629–642.
- Guamét, J.J. and Gianibelli, M.C. (1996) Nuclear and cytoplasmic 'stay green' mutations of soybean alter the loss of leaf soluble proteins during senescence. *Physiol. Plant.* **96**, 655–661.
- Guamét, J.J., Schwartz, E., Pichersky, E. and Noodén, L.D. (1991) Characterization of cytoplasmic and nuclear mutations affecting chlorophyll and chlorophyll-binding proteins during senescence in soybean. *Plant Physiol.* **96**, 227–231.
- Hendry, G.A., Houghton, J.D. and Brown, S.B. (1987) The degradation of chlorophyll – a biological enigma. *New Phytol.* **107**, 255–302.
- Hidema, J., Makino, A., Mae, T. and Ojima, K. (1991) Photosynthetic characteristics of rice leaves aged under different irradiances from full expansion through senescence. *Plant Physiol.* **97**, 1287–1293.
- Hidema, J., Makino, A., Kurita, Y., Mae, T. and Ojima, K. (1992) Changes in the levels of chlorophyll and light-harvesting chlorophyll *a/b* protein of PSII in rice leaves aged under different irradiances from full expansion through senescence. *Plant Cell Physiol.* **33**, 1209–1214.
- Hörtensteiner, S. (2006) Chlorophyll degradation during senescence. *Annu. Rev. Plant Biol.* **57**, 55–77.
- Hörtensteiner, S. and Feller, U. (2002) Nitrogen metabolism and remobilization during senescence. *J. Exp. Bot.* **53**, 927–937.
- Hwang, Y., Bethke, P.C., Gubler, F. and Jones, R.L. (2003) cPrG-HCl, a potential H⁺/Cl⁻ symporter, prevents acidification of storage vacuoles in aleurone cells and inhibits GA-dependent hydrolysis of storage proteins and phytate. *Plant J.* **35**, 154–163.
- Inskip, W.P. and Bloom, P.R. (1985) Extinction coefficients of chlorophyll *a* and *b* in *N,N*-dimethylformamide and 80% acetone. *Plant Physiol.* **77**, 483–485.
- Iriyama, K., Ogura, N. and Takamiya, A. (1974) A simple method for extraction and partial purification of chlorophyll from plant material, using dioxane. *J. Biochem.* **76**, 901–904.
- John, I., Drake, R., Farrell, A., Cooper, W., Lee, P., Horton, P. and Grierson, D. (1995) Delayed leaf senescence in ethylene-deficient ACC oxidase antisense tomato plants: molecular and physiological analysis. *Plant J.* **7**, 483–490.
- Kapri-Pardes, E., Naveh, L. and Adam, Z. (2007) The thylakoid lumen protease DegP1 is involved in the repair of photosystem II from photoinhibition in Arabidopsis. *Plant Cell*, **19**, 1039–1047.
- Kato, Y., Murakami, S., Yamamoto, Y., Chatani, H., Kondo, Y., Nakano, T., Yolota, A. and Sato, F. (2004) The DNA-binding protease, CND41, and the degradation of ribulose-1,5-bisphosphate carboxylase/oxygenase in senescent leaves of tobacco. *Planta*, **220**, 97–104.
- Kinoshita, T., Yamada, K., Hiraiwa, N., Kondo, M., Nishimura, M. and Hara-Nishimura, I. (1999) Vacuolar processing enzyme is up-regulated in the lytic vacuoles of vegetative tissues during senescence and under various stress conditions. *Plant J.* **19**, 43–53.
- Köhler, R.H., Cao, J., Zipfel, W.R., Webb, W.W. and Hanson, M.R. (1997) Exchange of protein molecules through connections between higher plant plastids. *Science*, **276**, 2039–2042.
- Kokubun, N., Ishida, H., Makino, A. and Mae, T. (2002) The degradation of the large subunit of ribulose-1,5-bisphosphate carboxylase/oxygenase into the 44 kDa fragment in the lysates of chloroplasts incubated in darkness. *Plant Cell Physiol.* **43**, 1390–1395.
- Krupinska, K. (2006) Fate and activities of plastids during leaf senescence. In *The Structure and Function of Plastids* (Wise, R.R. and Hooper, J.K., eds). The Netherlands: Springer, pp. 433–449.
- Kusaba, M., Ito, H., Morita, R. et al. (2007) Rice NON-YELLOW COLORING 1 is involved in light-harvesting complex II and grana degradation during leaf senescence. *Plant Cell*, **19**, 1362–1375.
- Martínez, D.E., Bartoli, C.G., Grbic, V. and Guamét, J.J. (2007) Vacuolar cysteine proteases of wheat (*Triticum aestivum* L.) are common to leaf senescence induced by different factors. *J. Exp. Bot.* **58**, 1099–1107.
- Martínez, D.E., Costa, M.L. and Guamét, J.J. (2008) Senescence associated degradation of chloroplast proteins inside and outside the organelle. *Plant Biol.* **10**, 15–22.
- Matile, P. (1997) The vacuole and cell senescence. *Adv. Bot. Res.* **25**, 87–112.
- Moriyasu, Y. (1995) Examination of the contribution of vacuolar proteases to intracellular protein degradation in *Chara corallina*. *Plant Physiol.* **109**, 1309–1315.
- Nakabayashi, K., Ito, M., Kiyosue, T., Shinozaki, K. and Watanabe, A. (1999) Identification of *clp* genes expressed in senescing Arabidopsis leaves. *Plant Cell Physiol.* **40**, 504–514.
- Nakano, T., Nagata, N., Kimura, T. et al. (2003) CND41, a chloroplast nucleoid protein that regulates plastid development, causes reduced gibberellin content and dwarfism in tobacco. *Physiol. Plant.* **117**, 130–136.
- Noodén, L.D., Guamét, J.J. and John, I. (2004) Whole plant senescence. In *Plant Cell Death Processes in Plants* (Noodén, L.D., ed.). San Diego, CA: Academic Press, pp. 227–244.
- Otegui, M., Noh, Y.S., Martínez, D.E., Vila Petroff, M.G., Staehelin, L.A., Amasino, R. and Guamét, J.J. (2005) Senescence-associated vacuoles with intense proteolytic activity develop in leaves of Arabidopsis and soybean. *Plant J.* **41**, 831–844.
- Park, H., Eggink, L.L., Roberson, R.W. and Hooper, J.K. (1999) Transfer of proteins from the chloroplast to vacuoles in *Chlamydomonas reinhardtii* (Chlorophyta): a pathway for degradation. *J. Phycol.* **35**, 528–538.
- Scarpeci, T.E., Marro, M.L., Bortolotti, S., Boggio, S.B. and Valle, E.M. (1997) Plant nutritional status modulates glutamine synthetase levels in ripe tomatoes (*Solanum lycopersicum* cv. Micro-Tom). *J. Plant Physiol.* **164**, 137–145.
- Schmid, M., Simpson, D.J. and Gietl, C. (1999) Programmed cell death in castor bean endosperm is associated with the accumulation and release of a cysteine endopeptidase from ricinosomes. *Proc. Natl Acad. Sci. USA*, **96**, 14159–14164.

- Smart, C.M., Hosken, S.E., Thomas, H., Greaves, J.A., Blair, B.G. and Schuch, W.** (1995) The timing of maize leaf senescence and characterization of senescence-related cDNAs. *Physiol. Plant.* **93**, 673–682.
- Swanson, S.J., Bethke, P.C. and Jones, R.L.** (1998) Barley aleurone cells contain two types of vacuoles: characterization of lytic organelles by use of fluorescent probes. *Plant Cell*, **10**, 685–698.
- Szumilo, T., Kaushal, G.P., Hori, H. and Elbein, A.** (1986) Purification and properties of a glycoprotein processing α -mannosidase from mung bean seedlings. *Plant Physiol.* **81**, 383–389.
- Takamiya, K.-i., Tsuchiya, T. and Ohta, H.** (2000) Degradation pathway(s) of chlorophyll: what has gene cloning revealed? *Trends Plant Sci.* **5**, 426–431.
- Thomas, H. and Howarth, C.J.** (2000) Five ways to stay green. *J. Exp. Bot.* **51**, 329–337.
- Tollenaar, M. and Wu, J.** (1999) Yield improvement in temperate maize is attributable to greater stress tolerance. *Crop Sci.* **39**, 1597–1604.
- Zelisko, A., García-Lorenzo, M., Jackowski, G., Jansson, S. and Funk, C.** (2005) AtFtsH6 is involved in the degradation of the light-harvesting complex II during high-light acclimation and senescence. *Proc. Natl Acad. Sci. USA*, **102**, 13690–13704.
- Zhang, L.F., Rui, Q., Zhang, P., Wang, X.Y. and Xu, L.L.** (2007) A novel 51 kDa fragment of the large subunit of ribulose-1,5-bisphosphate carboxylase/oxygenase formed in the stroma of chloroplasts in dark-induced senescing wheat leaves. *Physiol. Plant.* **131**, 64–71.